A., 1990; pp 86-124.
21. *Selectophore: Ionophores for Ion-Selective Electrodes and Optodes*; Fluka Chemie AG: Buchs, Switzerland, 1991; p 40.
22. Lee, K. S.; Shin, J. H.; Han, S. H.; Cha, G. S.; Shin, D. S.; Kim, H. D. *Anal. Chem.* **1993**, *65*, 3151.
23. Koryta, J.; Stulik, *K Ion-Selective Electrodes*; Cambridge University Press: Cambridge, England, 1983; p 77.
24. Cotton, F. A.; Wilkinson, G. *Advanced Inorganic Chemistry*, 5th Ed.; John Wiley & Sons: New York, U. S. A., 1988; p 693.

MO Studies on C_{60} and Its Pt-Derivatives

Kee Hag Lee, Han Myoung Lee, and Wang Ro Lee

Department of Chemistry, WonKwang University, Iri 570-749, Korea
Received November 2, 1994

The electronic structures of the C_{60}, $(H_3P)_2Pt(\eta^2\text{-}C_2H_4)$ and $(H_3P)_2Pt(\eta^2\text{-}C_{60})$ are calculated by using the EHMO method with the fragment analysis. We have modified the EHT parameters so as to yield the orbital energy level correlation and to fit the optical transition gap to the previous theoretical results of C_{60}. In Pt-derivatives, our FMO results with the modified parameters show that the carbon-carbon double bonds of C_{60} and ethene react like those of electron-poor arenes and alkenes, and also that C_{60} is more electron-susceptive than C_2H_4.

Introduction

In 1985, a soccer ball carbon structure, C_{60} or BF (Buckminsterfullerene), was obtained through laser vaporization of graphite in a high-pressure supersonic nozzle (Smalley *et al.*[1]). Since the development of the large-scale synthesis of fullerenes, a variety of studies of the cluster have been promoted in order to discern chemical and physical properties.[2,3] The stability of the C_{60} has been calculated using MNDO,[4] *ab initio* SCF[5] and Hückel[6] methods. The 3D-Hückel,[7] DV-Xα[8] and Linear Muffin-Tin Orbitals (LMTO)[9] calculations have been represented for the orbital energy levels of this compound.

The interaction of fullerenes with molecules has been of fundamental interest, so several papers showed the chemical reactivity between metal (Os, Pt, Ir) complexes and C_{60} *via* solution chemistry forming metal-C_{60} bonds. Hawkins *et al.*[10] have synthesized a one-to-one C_{60}-osmium tetroxide adduct, $C_{60}(OsO_4)$(4-*tert*-butylpyridine)$_2$, in which osmium was connected through a pair of oxygen atoms to the exterior of the C_{60}.

Balch *et al.*[11] have shown that addition of an equimolar amount of a purple solution of C_{60} in benzene to a yellow benzene solution of $Ir(CO)Cl(PPh_3)_2$ immediately forms a deep brown solution from which black-brown crystals of $(\eta^2\text{-}C_{60})Ir(CO)Cl(PPh_3)_2 \cdot 5C_6H_6$ precipitate.

Fagan *et al.*[13] have shown that the addition of C_{60} to $(Ph_3P)_2Pt(\eta^2\text{-}C_2H_4)$ results in displacement of ethylene and formation of $(\eta^2\text{-}C_{60})Pt(PPh_3)_2$. For the platinum complex $[(C_6H_5)_3P]_2Pt(\eta^2\text{-}C_{60})$, the reactivity of C_{60} is not like that of relatively electron-rich planar aromatic molecules such as benzene, that is, the carbon-carbon double bonds of C_{60} behave chemically like those of very electron-deficient arenes and alkenes. In terms of the platinum coordination sphere, it was found that this C_{60} complex formed at the junction of two fused 6-MRs in C_{60} closely resembles the structures seen for other platinum alkene complex,[13b] $[(C_6H_5)_3P]_2Pt(\eta^2\text{-ethylene})$. Also, using NMR spectra and X-ray crystalographic results of the hexa-substituted platinum derivative $\{[(C_6H_5)_3P]_2Pt\}_6C_{60}$, Fagan *et al.*[14] have shown that the molecule has a multiply-substituted buckminsterfullerene with an octahedral array of platinum atoms.

Their structural studies for metal complexation suggest that the bonds between two fused six-membered rings in C_{60} are the most reactive, these bonds being shorter and having the most double bond character. The fact that low-valent metal centers like Ir(I) and Pt(0) add to the carbon atoms at 6-6 membered ring fusions in C_{60} was consistent with the predictions of bond localization energy calculations.[12]

Fann *et al.*[15] have calculated for C_{60} and the bunnyballs (Os-C_{60}, Ru-C_{60} and Mn-C_{60} complexes) by the Extended Hückel (EH) method. The energy level correlation of C_{60} in his work is similar to Figure 1 in this paper, but it is very different from those of 3D-Hückel,[7] DV-Xα,[8] and CNDO/S.[3] *Ab initio* molecular orbital calculations[18] for $(\eta^2\text{-}C_2H_4)Pt(PH_3)_2$ and $(\eta^2\text{-}C_{60})Pt(PH_3)_2$ have shown that charge transfer from Pt fragment is 0.347 to C_2H_4 and 0.926 to C_{60}, and binding energy (eV) with $Pt(PH_3)_2$ is 0.32 for C_2H_4 and 0.95 for C_{60}.

Therefore, it suggests that it is interesting and important to choose proper EH parameters for calculations of the intermediate size cage cluster like C_{60} between molecule and surface. EH method with and without Carbon parameter modification is used to see a detailed molecular orbital (MO) description of the effect of addition of C_{60} to $(Ph_3P)_2Pt(\eta^2\text{-ethylene})$ which results in displacement of ethylene and formation of $(\eta^2\text{-}C_{60})Pt(PPh_3)_2$. All calculations are simplified by substituting the phenyl groups (C_6H_5-) in each complex with hydrogen atoms.

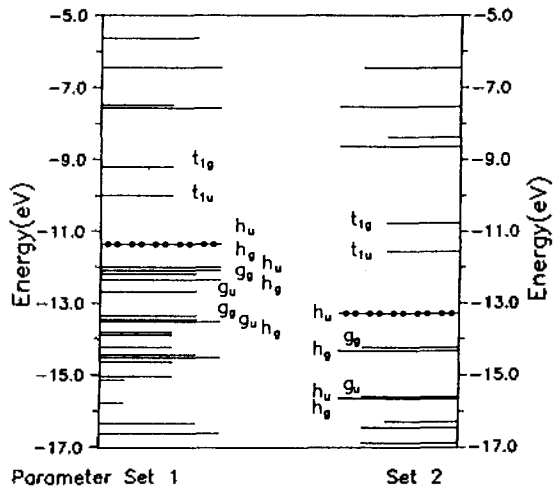

Figure 1. Energy level correlation of C_{60} with EHT parameter set **1** and **2** (all bond lengths of C_{60} are 1.421 Å).

Calculations

First, using the EHMO method, we have calculated the electronic structure for the C_{60}. We use the previous parameters of carbon[16] which are mainly used for molecules containing small amounts of carbon. The Hückel constant (K) is 1.75, and the 2s and 2p orbital exponents and ionization potentials are 1.625, −21.4 eV, and 1.625, −11.4 eV, respectively. This is called parameter set **1** in this paper. Our results show that the energy level correlation near the HOMO-LUMO energy levels of C_{60} differs from the results of the other theoretical studies; 3D-HMO,[7] DV-Xα[8] and LMTO[9] calculations. Thus, we have modified the previous parameters for the carbon cluster by comparing our results with the energy level correlations near the HOMO and the LUMO states of others and by fitting the optical transition to the DV-Xα result which comparatively agrees with the experimental studies (see Figure 1). The modified parameter set is as follows; K=2.35, exp(p)=1.92, and VSIP(p)= −12.67 eV. Here the K value within a specific distance (R) is almost the same as the value of K_1 exp($-K_2R$) factor for the modified off-diagonal elements which are used in modified EH band calculations on conjugated polymers.[17] In the modified parameter set, parameters of *s*-orbital of carbon are the same with parameter set **1** except the K-value.

Secondly, we have performed EHMO calculations of the complex, $(H_3P)_2Pt(\eta^2\text{-}C_{60})$. Also MO calculations of the well-known complex $(H_3P)_2Pt(\eta^2\text{-}C_2H_4)$ are done for a review of orbital interactions for typical olefin-metal complex. The result is compared with those of two different types of Pt-C_{60} complexes. The two different types of complexes of $(H_3P)_2Pt(\eta^2\text{-}C_{60})$ are as follows: one formed by addition of Pt-ligand to a junction of two 6-MRs (6-6MRs) of C_{60}; another formed by addition of Pt-ligand to a junction of 5- and 6-MRs (5-6MRs) of C_{60}. Both are considered as Pt-derivatives of C_{60}.

The structure used in these calculations was taken from the crystal structure[13] for the platinum complex $[(C_6H_5)_3P]_2Pt(\eta^2\text{-}C_{60})\cdot C_4H_8O$, and thus small deviation from the icosahedral symmetry is observed. The distances and the bond angles around platinum in $(H_3P)_2Pt(\eta^2\text{-}C_2H_4)$ and $(H_3P)_2Pt(\eta^2\text{-}C_{60})$ are shown in Figure 2. But any experimental study of the complex formed by addition of Pt-ligand to a fusion of 5-6MRs of C_{60} was not reported. With the assumption that the difference of structures between two types of Pt-C_{60} complex is not serious, the geometries of "free" C_{60} and Pt-ligand obtained from X-ray analysis of $(Ph_3P)_2Pt(\eta^2\text{-}C_{60})$ complex formed at a fusion of 6-6MRs of C_{60} are used. Thus the variations of bond length at a fusion of 5-6MRs of C_{60} effected by Pt-ligand are not considered.

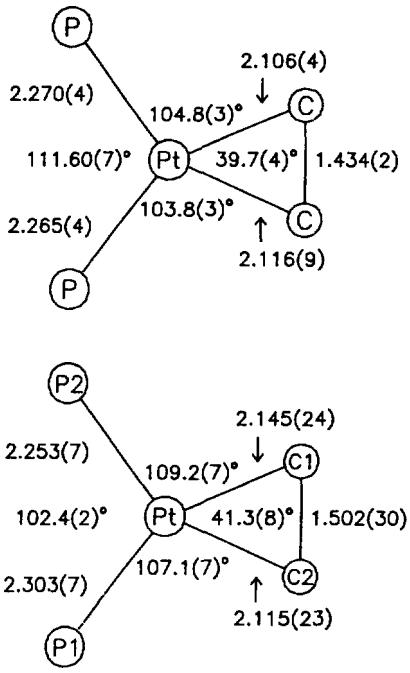

Figure 2. Comparison of the Pt coordination spheres in $(H_3P)_2Pt(\eta^2\text{-}C_2H_4)$(upper)[13b] and $(H_3P)_2Pt(\eta^2\text{-}C_{60})$(lower).[13a]

Table 1. Parameters Used in EHMO Calculations of Hydrogen, Phosphine and Platinum[16]

	s			*p*			*d*					
	n	IP	ζ	*n*	IP	ζ	*n*	IP	ζ_1	ζ_2	c_1	c_2
H	1	13.6	1.3									
P	3	18.6	1.75	3	14.0	1.3						
Pt	6	9.077	2.554	6	5.475	2.554	5	12.59	6.013	2.696	0.6334	0.5513

The previous parameter set (parameter set **1**) and the modified parameter set (parameter set **2**) are used in EHMO calculations of these complexes. The previous parameters of the other atoms (H, P and Pt) in these complexes are shown in Table 1, which are not changed in this work. The fragment molecular orbital (FMO) calculations for $(H_3P)_2Pt(\eta^2\text{-}C_{60})$ with fragments, η^2-C_{60} and $Pt(PH_3)_2$, and for $(H_3P)_2Pt(\eta^2\text{-}C_2H_4)$ with fragments, η^2-C_2H_4 and $Pt(PH_3)_2$, give orbital interaction diagrams as shown in Figures 3-5.

Results and Discussion

Table 2 shows the charge of $Pt(PH_3)_2$ fragment in each complex, the charge variations of Pt in Pt-ligand and Pt-de-

Table 2. Results from EH-FMO Calculations for $(H_3P)_2Pt(\eta^2$-$C_2H_4)$ and $(H_3P)_2Pt(\eta^2$-$C_{60})$ with Each Parameter Set

	Parameter Sets	HOMO-LUMO gap(eV) $(H_3P)_2Pt$	R	$(H_3P)_2Pt(\eta^2$-R)	Charge transfer	Δq^a of Pt	BE[b]
$(H_3P)_2Pt$-	1	4.93	3.98	4.83	0.292	0.273	0.89
$(\eta^2$-$C_2H_4)$	2	5.11	4.98	5.27	0.474	0.444	3.99
$(H_3P)_2Pt$-	1	4.62	1.48	1.29	0.303	0.272	0.44
$(\eta^2$-$C_{60})$,							
(at 6-6MR)	2	4.73	1.88	0.51	0.801	0.713	4.23
$(H_3P)_2Pt$-	1	4.62	1.60	0.90	0.255	0.246	0.12
$(\eta^2$-$C_{60})$,							
(at 5-6MR)	2	4.73	2.07	0.49	1.143	1.039	3.34

R = C_2H_4 or C_{60}. a = Charge of Pt in $(H_3P)_2Pt(\eta^2$-R) - Charge of Pt in $Pt(PH_3)_2$. b = Fragment Energies of $(H_3P)_2Pt$ and R - Energy of Complex.

rivatives, and the energy gap differences between the HOMO and the LUMO in complexes and each fragment.

In the aspect of stabilization energy for formation of complex from the fragments, the complex in which Pt-ligand is attached to the junction of two 6-MRs of C_{60} is less stable than the complex $(PH_3)_2Pt(\eta^2$-$C_2H_4)$, when we use the parameter set **1**. But when we use the parameter set **2**, the reverse stability is obtained. The experimental result suggests that $(PH_3)_2Pt(\eta^2$-$C_{60})$ may be more stable than $(PH_3)_2Pt(\eta^2$-$C_2H_4)$. The EHMO result with parameter set **2** can explain the experimental result from addition of C_{60} to $(Ph_3P)_2Pt(\eta^2$-ethylene), which displaces ethylene and forms $(\eta^2$-$C_{60})Pt(PPh_3)_2$ at 6-6MRs of C_{60}. Therefore, it suggests that we must be very careful to choose the EHT-parameters for the big cage clusters like C_{60}.

The binding energies (BE) from calculations by using parameter set **2** show that $(H_3P)_2Pt(\eta^2$-$C_{60})$ formed by addition of Pt-ligand to a junction of 6-6MRs of C_{60} is the most stable. Calculations with both parameter sets show that Pt-C_{60} complex with Pt-ligand attached at the junction of 6-6 MRs of C_{60} is more stable than is Pt-C_{60} complex with Pt-ligand attached at the junction of 5-6 MRs of C_{60}. The difference of the binding energy between two Pt-C_{60} type complexes, using parameter set **2**, is about 1 eV. It suggests that the Pt-fragment attaches the carbon atoms at the junction of 6-6MRs of C_{60} as in the X-ray crystal results.[13]

In parameter set **2** case, the total Mulliken charge of the $Pt(PH_3)_2$ fragment in $(\eta^2$-$C_{60})Pt(PH_3)_2$ is 0.80: strong electron back-donation from $Pt(PH_3)_2$ to C_{60} takes place, but total Mulliken charge of the $Pt(PH_3)_2$ fragment in $(\eta^2$-$C_2H_4)Pt(PH_3)_2$ is 0.47: it is 59% of that in the C_{60} fragment. Meanwhile, in parameter set **1** case, the total Mulliken charge of each $Pt(PH_3)_2$ fragment in both of $(\eta^2$-$C_{60})Pt(PH_3)_2$ and $(\eta^2$-$C_2H_4)Pt(PH_3)_2$ complexes is almost the same (~0.3). From the charges of Pt ligand, the electron acceptance of ethylene and C_{60} is stronger using parameter set **2** than is that using parameter set **1**. The electron acceptance (~0.8) of C_{60} with parameter set **2** is almost the same to *ab initio* result[18] (~0.9). The C_{60} is more electron-acceptive than ethylene. The origin of electron gain on C_{60} and C_2H_4 shown in Table 2 is mainly from the Pt *d*-orbitals.

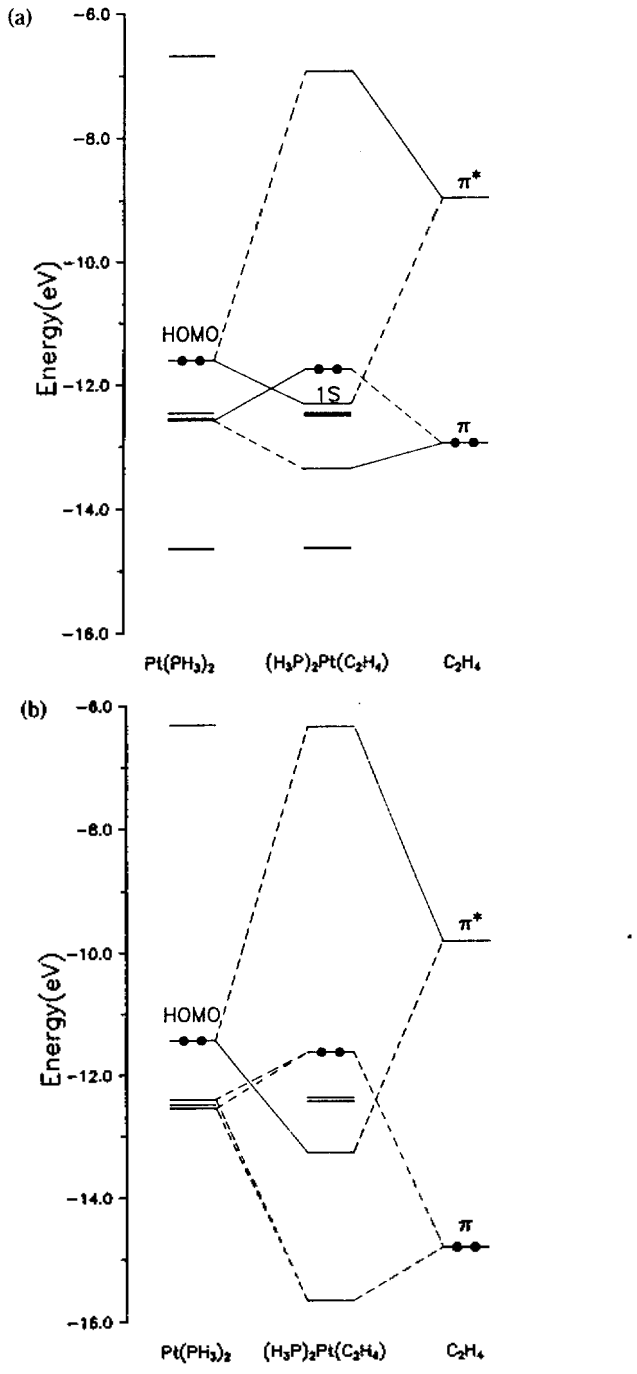

Figure 3. Molecular orbital interaction diagrams of $(H_3P)_2Pt(\eta^2$-$C_2H_4)$, (a) with the (previous) parameter set **1** and (b) with the (modified) parameter set **2**. Here 1S means the MO energy level of Scheme 1.

The HOMO-LUMO energy splitting for "free" C_{60} and C_2H_4 is larger in parameter set **2** than in set **1**. The orbital interaction of the HOMO of Pt-ligand and the LUMO of C_{60} (or C_2H_4) is larger in parameter set **2** than in set **1**, as shown in Figures 3-5. The HOMO-LUMO energy splitting in both of two Pt-C_{60} type complexes is smaller than "free" C_{60}. The HOMO-LUMO energy splitting of $(H_3P)_2Pt(\eta^2$-$C_2H_4)$ is larger than that of "free" C_2H_4. It is explained as both of the HOMO and the LUMO in Pt-C_2H_4 are antibonding MOs, but

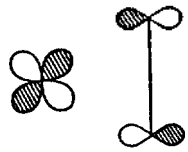

Scheme 1.

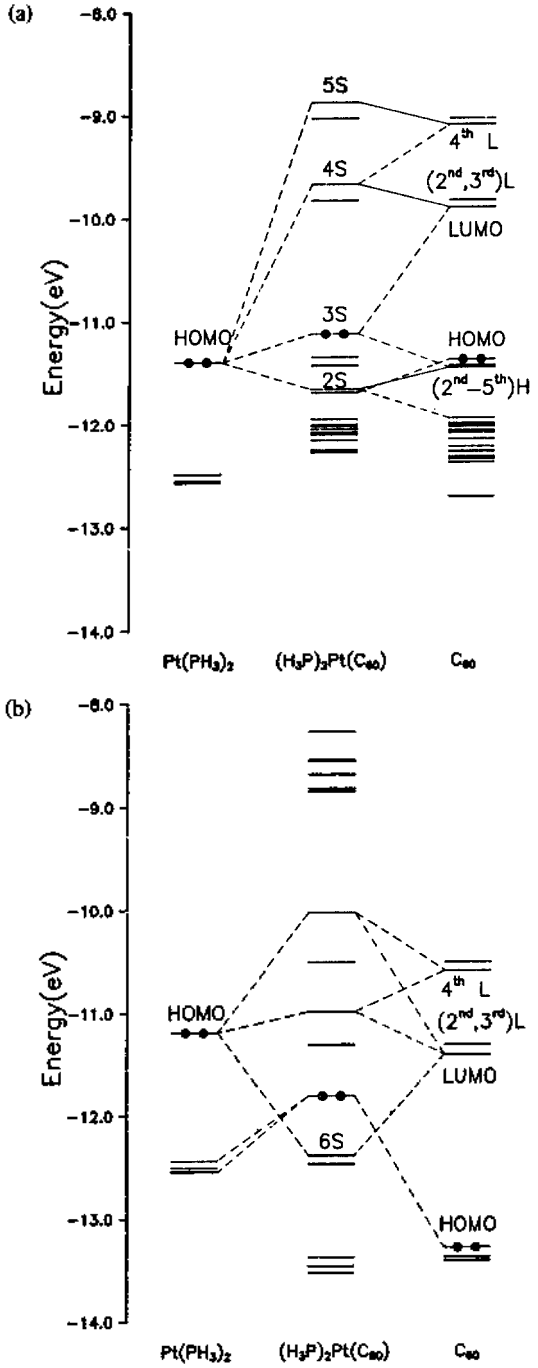

Figure 4. Molecular orbital interaction diagrams of $(H_3P)_2Pt(\eta^2\text{-}C_{60})$ formed by addition of Pt-ligand to a junction of two 6-MRs of C_{60}, (a) with the (previous) parameter set 1 and (b) with the (modified) parameter set 2. Here numbered H(L) means the n^{th} HOMO (LUMO), and numbered S means the MO energy level of Scheme number.

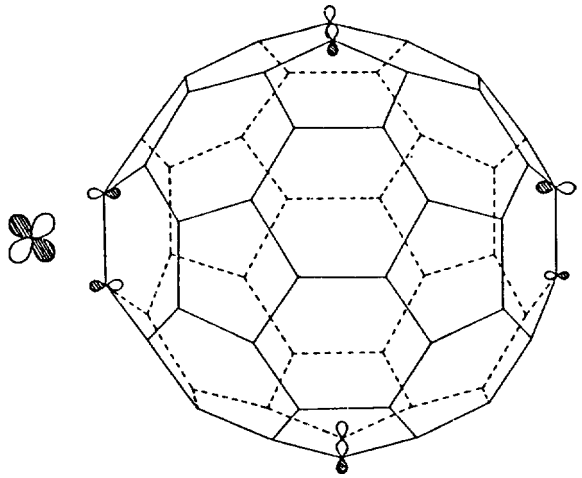

Scheme 2.

in Pt-C_{60} the HOMO is antibonding character and the LUMO is nonbonding orbital mainly due to contributions of nonbonding fragment orbitals from the C_{60}, *i.e.* the HOMO-LUMO energy splitting in C_{60} is apparently compressed in Pt-C_{60}. The variation of the HOMO-LUMO energy splitting in both of parameter set 1, 2 shows the same tendency.

Since the structure was generated from real crystal structure, there are no symmetry correlation in the orbital interaction diagrams by the FMO calculations of $(H_3P)_2Pt(\eta^2\text{-}C_2H_4)$ and $(H_3P)_2Pt(\eta^2\text{-}C_{60})$, thus no depicting orbital symmetry labels in Figures 3-5. But, since the phosphorus, platinum, and carbon atoms are closely associated with C_{2v} point group symmetry, fragment orbital interactions are drawn in Schemes 1-9.

In Figure 3 for $(H_3P)_2Pt(\eta^2\text{-}C_2H_4)$, Figure 3(a) represents the result using parameter set 1, and Figure 3(b) represents that using set 2.

In Figure 3(a) nonbonding metal orbital which is the HOMO of Pt-fragment has the approximate symmetry to match that of the π^*-orbital of ethylene as shown in Scheme 1. The HOMO of Pt-fragment is stabilized by π^*, an electron-acceptor of ethylene. Through this interaction of Pt-fragment and ethylene, electron is transferred from Pt-ligand to ethylene. Also there is a two-orbital, four-electron interaction between an electron-filled π orbital of ethylene and an electron-filled orbital of Pt-fragment. This repulsive interaction is too small to affect the destabilization of the complex. The diagram in Figure 3(b) shows only the interaction between the HOMO of Pt-fragment and the π^* orbital of ethylene. The energy gap between the HOMO of Pt-fragment and the π^* orbital of ethylene is considerably smaller in Figure 3(b) than in Figure 3(a). So the interaction is stronger in Figure 3(b) than in Figure 3(a), that is, the electron-donor effect of this orbital interaction is stronger in Figure 3(b) than in Figure 3(a). Also, the stability of this orbital interaction obtained by using parameter set 2 is larger than is that of parameter set 1.

The FMO calculations have been performed for the complex in which Pt-ligand was added to the junction of 6-6MRs of C_{60}, as it was for $(H_3P)_2Pt(\eta^2\text{-}C_2H_4)$. The orbital interaction diagrams are quite tangled as shown in Figure 4.

In Figure 4(a) with parameter set 1, the orbital interaction

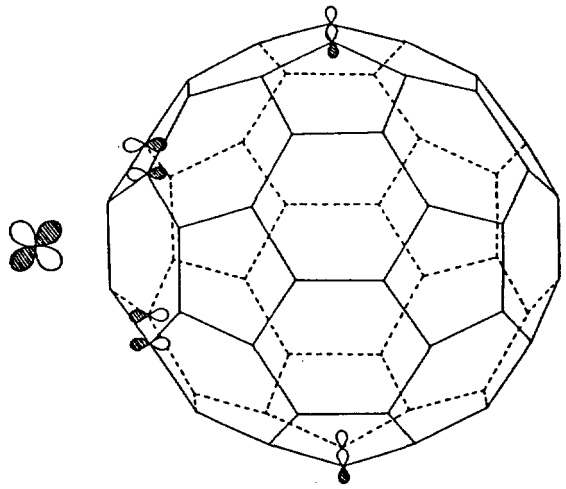

Scheme 3.

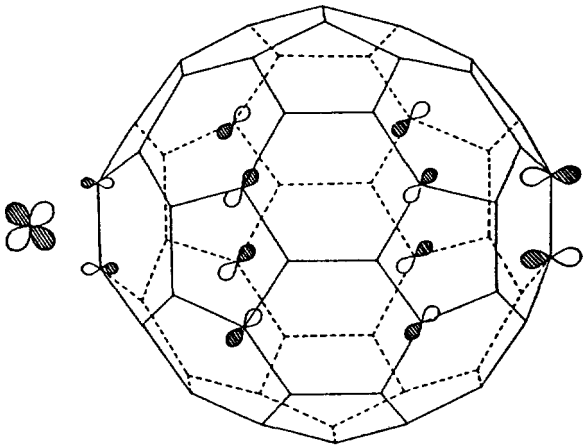

Scheme 4.

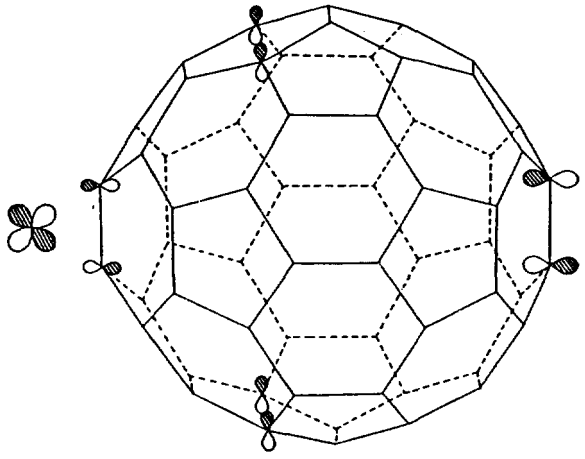

Scheme 5.

between the 5th HOMO of C_{60} and the HOMO of the fragment of $Pt(PH_3)_2$ forms a bonding MO (see Scheme 2) at an energy lower than the HOMO of Pt-C_{60} complex and an antibonding HOMO (see Scheme 3) of Pt-C_{60} complex. The HOMO of Pt-C_{60} complex is mainly composed of 40% of the 5th HOMO of C_{60} and 30% of the HOMO of $Pt(PH_3)_2$ fragment. The

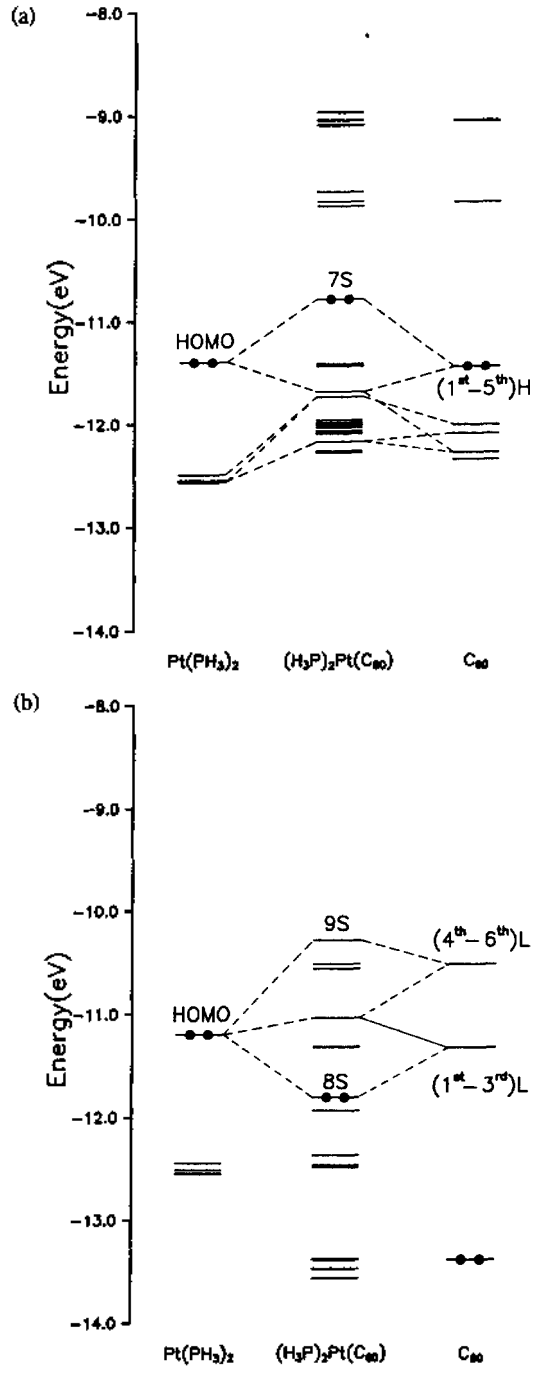

Figure 5. Molecular Orbital Interaction diagrams of $(H_3P)_2Pt(\eta^2$-$C_{60})$ formed by addition of Pt-ligand to a junction of 5- and 6-MRs of C_{60}, (a) with the (previous) parameter set **1** and (b) with the (modified) parameter set **2**. Here numbered H(L) means the nth HOMO (LUMO), and numbered S means the MO energy level of Scheme number.

HOMO energy level of Pt-C_{60} complex is higher than the HOMO energy of each fragment, which is contrary to the result for $(H_3P)_2Pt(\eta^2$-$C_2H_4)$. Antibonding interactions of the HOMO orbital of Pt-fragment with both the LUMO and the 4th LUMO of C_{60} make up unoccupied molecular orbitals as shown in Schemes 4 and 5, repectively.

In Figure 4(b) with parameter set **2**, interaction of the

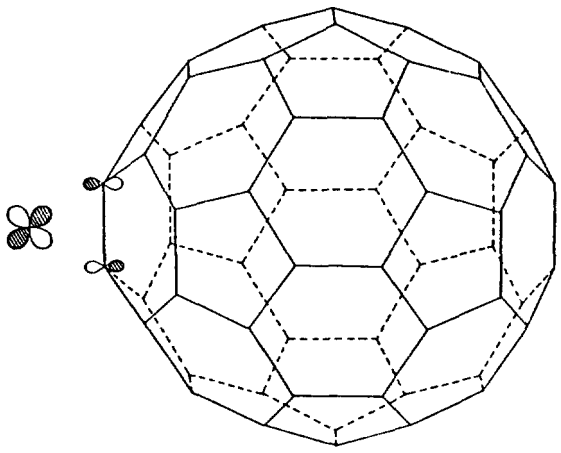

Scheme 6.

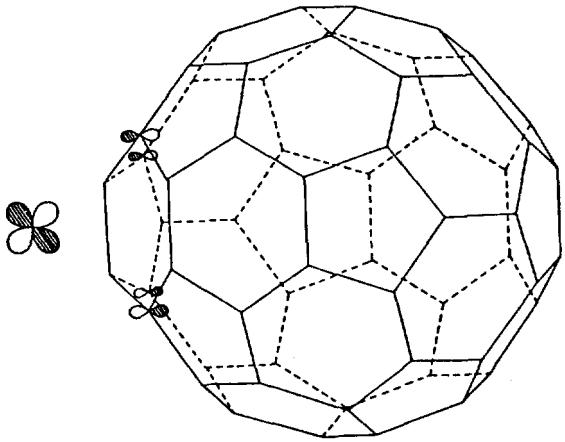

Scheme 7.

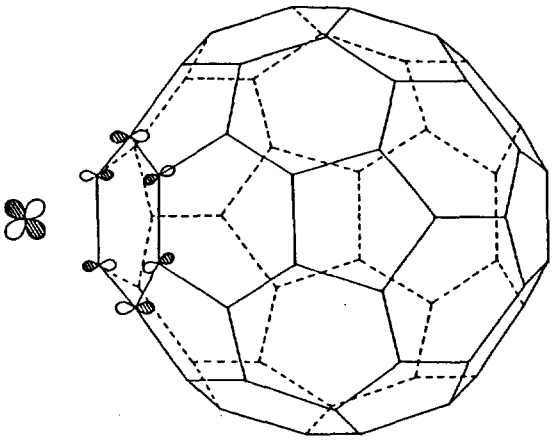

Scheme 8.

HOMO of Pt-fragment with the LUMO of C_{60} forms a bonding molecular orbital as shown in Scheme 6, in which the HOMO of Pt-fragment is stabilized as electron-donor to the LUMO of C_{60} fragment.

Figure 5 is the orbital interaction diagram for Pt-derivative with approximate C_s point group, which is formed with Pt-ligand attaching to a junction of 5-6MRs of C_{60}. In Figure 5(a) with parameters set **1**, the HOMO of Pt-fragment interacts with the 3rd and the 4th HOMOs of C_{60} to form the HOMO of Pt-C_{60} as shown in Scheme 7. It is destabilizing and repulsive since interaction is a two-orbital, four electron one.

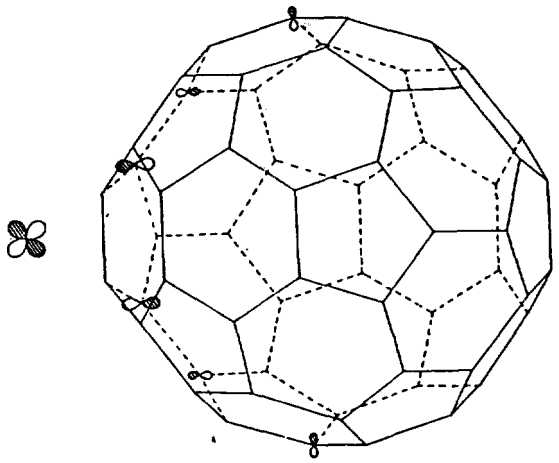

Scheme 9.

The result from FMO calculation with parameter set **2** is shown in Figure 5(b). The orbital interaction between the HOMO of Pt-fragment and the LUMO of C_{60} constructs a bonding orbital of the complex as shown in Scheme 8. This orbital interaction also forms an antibonding 6th LUMO of Pt-C_{60} complex as shown in Scheme 9.

In the two different Pt-C_{60} type complexes as shown in Table 2, the electron acceptance of C_{60} from Pt-ligand is larger using the parameter set **2** than using parameter set **1**. The electron acceptance of buckminsterfullerene with parameter set **2** is weaker in one type of Pt-C_{60} complex formed by attachment of Pt-ligand to the carbon atoms at the junction of 6-6MRs of C_{60} than in another type complex which has Pt-ligand added to the carbon atoms at the 5-6MRs fusions of C_{60}.

In conclusion, when we compare our results with *ab initio*[18] and experimental[13] results, our results are better using parameter set **2** than using parameter set **1**. The absolute value of binding energy (set **2**) is physically unreasonable, but the difference of BE between the C_{60}- and the C_2H_4-derivatives is meaningful. The HOMO of Pt-fragment interacts with unoccupied molecular orbitals of C_{60} or ethylene, which is stabilized by transfering its electrons to unoccupied fragment molecular orbitals of C_{60} or C_2H_4. Our results for the $(H_3P)_2$-Pt(η^2-C_2H_4) and $(H_3P)_2$Pt(η^2-C_{60}) show that the carbon-carbon double bonds of C_{60} and ethene react like those of electron-poor arenes and alkenes, and also that C_{60} is more electron-susceptive than C_2H_4.

Acknowledgment. This research was supported through KOSEF grant 90-030003 and 94-080011013.

References

1. Kroto, H. W.; Heath, J. R.; O'Brien, S. C.; Curl, R. F.; Smalley, R. E. *Nature* **1985**, *318*, 162.
2. Kroto, H. W.; Allaf, A. W.; Balm, S. P. *Chem. Rev.* **1991**, *91*, 1213 and references within.
3. Sydney Leach; Michel Vervloet; Alain Despres; Emilienne Breheret; Hare, J. P.; Dennis, T. J.; Kroto, H. W.; Roger Taylor; Walton, D. R. M. *Chem. Phys.* **1992**, *160*,

451.
4. Newton, M. D.; Stanton, R. E. *J. Am. Chem. Soc.* **1986**, *108*, 2469.
5. Lüthi, H. P.; Almlöf, J. *Chem. Phys. Lett.* **1987**, *135*, 357.
6. Ozaki, M.; Takahashi, A. *Chem. Phys. Lett.* **1986**, *127*, 242.
7. Haddon, R. C.; Brus, E. L.; Raghavachari, K. *Chem. Phys. Lett.* **1986**, *125*, 459.
8. Hale, P. D. *J. Am. Chem. Soc.* **1986**, *108*, 6087.
9. Sashi Satpathy *Chem. Phys. Lett.* **1986**, *130*, 545.
10. Hawkins, J. M.; Meyer, A.; Lewis, T. A.; Stefan Loren; Hollander, F. J. *Science* **1991**, *252*, 312.
11. Balch, A. L.; Catalano, V. J.; Lee, J. W. *Inorg. Chem.* **1991**, *30*, 3980.
12. Amié, D.; Trinajstip *J. Chem. Soc., Perkin Trans.* **1990**, *2*, 1595.
13. (a) Fagan, P. J.; Calabrese, J. C.; Brian Malone *Science* **1991**, *252*, 1160. (b) Cheng, P.-T.; Nyburg, S. C. *Can. J. Chem.* **1972**, *50*, 912.
14. Fagan, P. J.; Calabrese, J. C.; Brian Malone *J. Am. Chem. Soc.* **1991**, *113*, 9408.
15. Fann, Y. C.; Singh, D.; Jansen, S. A. *J. Phys. Chem.* **1992**, *96*, 5817.
16. (a) Hoffmann, R. *J. Chem. Phys.* **1963**, *39*, 1397. (b) Summerville, R. H.; Hoffmann, R. *J. Am. Chem. Soc.* **1976**, *97*, 7240.
17. Hong, S. Y.; Marynick, D. S. *J. Chem. Phys.* **1992**, *96*, 5497.
18. Koga, N.; Morokuma, K. *Chem. Phys. Lett.* **1993**, *202*, 330.

Oscillator Strengths and Intensity Parameters of Ln(III) Complexes with 12-Crown-4 and 15-Crown-5 Ethers in Acetonitrile (Ln=Ho and Er)

Jun-Gill Kang*, Soo-Kyung Yoon, Eun-Jeong Kim, Jong-Gu Kim†, and Youn-Doo Kim

Department of Chemistry, Chungnam National University, Taejeon 305-764, Korea
†Radiochemistry Division, Korea Atomic Energy Research Institute, Taejeon 302-353, Korea
Received November 23, 1994

The absorption spectra of holmium nitrate and erbium nitrate and the difference absorption spectra of their complexes with crown ethers were measured in acetonitrile. The crown ethers used in this study are 12-crown-4 and 15-crown-5. The oscillator strengths for the $4f \rightarrow 4f$ multiplet-to-multiplet transitions are empirically determined from the absorption spectra in combination with the difference spectra. The intensity parameters Ω_λ ($\lambda=2, 4, 6$) for the systems are also evaluated by applying the Judd-Ofelt theorem to the observed oscillator strengths. The values of the intensity parameters are compared and discussed to investigate the sensitivity of the intensity parameters to the ligand environment.

Introduction

Lanthanides have been expected to form stable complexes similarly to alkaline and alkaline earth metals because of the similarity of the chemical bonding and the ionic radii between the lanthanides and Na^+ or Ca^{2+} ions. A great works dealing with the complexation of trivalent lanthanide ions, Ln(III), with macrocyclic ligands, specially crown ethers and their derivatives, have been performed to elucidate thermodynamic and kinetic properties of lanthanide complexes.[1] From a combination of conductivity,[2] IR[3] and NMR studies,[4] solvent extraction[5~7] and fluorescence[4,8] the most of studies have deduced the stoichiometry and stability and the cation-selectivity of lanthanide complexes with several crown ethers. However, despite the vast number of papers on crown ether complexes, there are little information on the absorption properties of the lanthanide complexes.[9]

Lanthanide(III) ions with $4f^N5s^25p^6$ show very characteristic $4f \rightarrow 4f$ absorption spectra which correspond to transitions from the ground multiplet to the excited multiplet. These transitions are forbidden in principle by an electric dipole moment, but are partially allowed by the induced electric dipole moment. Judd[10] and Ofelt[11] individually derived significant theoretical expressions for the oscillator strength of the induced electric dipole moment, taking into account the crystal-field potential causing the mixing between the $4f$ orbital and another orbital with an opposite parity. On the basis of the intermediate coupling scheme, the Judd-Ofelt theorem for the oscillator strength of the transition from the initial ΨJ to the final $\Psi' J'$ state is expressed as

$$P_{ED} = \chi\left(\frac{8\pi^2 mc\bar{\nu}}{h}\right) \sum_{\lambda=2,4,6} \Omega_\lambda \langle f^N;\ \Psi J \| U^{(\lambda)} \| f^N;\ \Psi' J' \rangle^2 (2J+1)^{-1} \quad (1)$$

where x is the Lorentz-field correction for the refractivity of the medium, m is the mass of an electron, and $\bar{\nu}$ is the transition energy given in cm^{-1}, $U^{(\lambda)}$ is an irreducible unit tensor operator of rank λ, and the bracket is the reduced

*To whom correspondence should be addressed.